Inorganic Chemistry

Article

pubs.acs.org/IC

Redox Energetics of *Hypercloso* Boron Hydrides B_nH_n (n = 6−13) and $B_{12}X_{12}$ (X = F, Cl, OH, and CH_3)

Tae Bum Lee and Michael L. McKee*

Department of Chemistry and Biochemistry, Auburn University, Auburn, Alabama 36849, United States

Supporting Information

ABSTRACT: The reduction potentials ($E°_{Red}$ versus SHE) of *hypercloso* boron hydrides B_nH_n (n = 6−13) and $B_{12}X_{12}$ (X = F, Cl, OH, and CH_3) in water have been computed using the Conductor-like Polarizable Continuum Model (CPCM) and the Solvation Model Density (SMD) method for solvation modeling. The B3LYP/aug-cc-pvtz and M06-2X/aug-cc-pvtz as well as G4 level of theory were applied to determine the free energies of the first and second electron attachment ($\Delta G_{E.A.}$) to boron clusters. The solvation free energies (ΔG_{solv}) greatly depend on the choice of the cavity set (UAKS, Pauling, or SMD) while the dependence on the choice of exchange/correlation functional is modest. The SMD cavity set gives the largest $\Delta\Delta G_{solv}$ for $B_nH_n^{0/-}$ and $B_nH_n^{-/2-}$ while the UAKS cavity set gives the smallest $\Delta\Delta G_{solv}$ value. The $E°_{Red}$ of $B_nH_n^{-/2-}$ (n = 6−12) with the G4/M06-2X(Pauling) (energy/solvation(cavity)) combination agrees within 0.2 V of experimental values. The experimental oxidative stability ($E_{1/2}$) of $B_nX_n^{2-}$ (X = F, Cl, OH, and CH_3) is usually located between the values predicted using the B3LYP and M06-2X functionals. The disproportionation free energies (ΔG_{dpro}) of $2B_nH_n^- \rightarrow B_nH_n + B_nH_n^{2-}$ reveal that the stabilities of $B_nH_n^-$ (n = 6−13) to disproportionation decrease in the order $B_8H_8^- > B_9H_9^- > B_{11}H_{11}^- > B_{10}H_{10}^-$. The spin densities in $B_{12}X_{12}^-$ (X = F, Cl, OH, and CH_3) tend to delocalize on the boron atoms rather than on the exterior functional groups. The partitioning of $\Delta G_{solv}(B_nH_n^{2-})$ over spheres allows a rationalization of the nonlinear correlation between $\Delta G_{E.A.}$ and $E°_{Red}$ for $B_6H_6^{-/2-}$, $B_{11}H_{11}^{-/2-}$, and $B_{13}H_{13}^{-/2-}$.

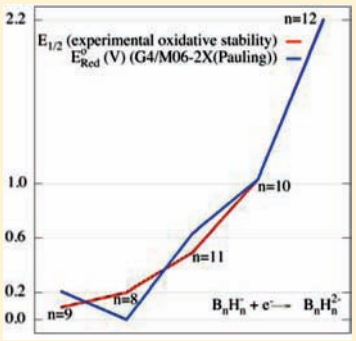

INTRODUCTION

Experimental studies of the electrochemistry of $B_nH_n^{-/2-}$ have been reported using polarography and cyclic voltammetry.[1] However, polymerization or aggregation of boron clusters during the redox reaction hinder the accurate characterization of redox species.[2] The existence of the assumed radical anions $B_{11}H_{11}^{\bullet-}$ and $B_{12}H_{12}^{\bullet-}$ depends on solvent, but the role of solvent itself is not well-known.[2d] For example, it is known that $B_{10}H_{10}^{2-}$ and $B_{12}H_{12}^{2-}$ undergo a stepwise one-electron oxidation to form $B_{20}H_{19}^{3-}$ or a two-electron oxidation to form $B_{20}H_{18}^{2-}$, depending on the solvent[3] and pH conditions.[4] Substitution of the $B_{12}H_{12}^{2-}$ opens the possible application of superacidity,[5] weakly coordinating systems,[6] biological labeling system,[7] and nanoscale pharmaceutical carrier.[8] However, the redox properties of $B_{12}X_{12}^{0/-/2-}$ (X = F, Cl, OH, CH_3, and OCH_3) have been only partially investigated.[6a,9] Lee et al.[9g] reported $E_{1/2}$ of $B_{12}(OR)_{12}^{0/-}$ where 16 different -OR substituents were considered from $-OCH_3$ to $-OCH_2C_6H_5Br$, while the $E_{1/2}$ of $B_nH_n^{0/-}$ and the existence of neutral B_nH_n is still not known.[2]

Many ab initio studies of reduction potentials have been reported in the past decade.[10] Roy et al.[10c] reported that the systematic underestimation of redox potentials with the B3LYP functional could be corrected with a baseline shift. The medium effect is often treated with implicit solvation models such as CPCM (Conductor-like Polarizable Continuum Model) which was successfully applied to the redox potential in aqueous and nonaqueous solution.[10b,e,h] The linear relationship between electron affinity and reduction potential is well-known, and a strong correlation is reported with various species.[10g,11] The difference between electron affinity and reduction potential comes from the consideration of the solvation Gibbs free energy (ΔG_{solv}) (Scheme 1).

The PCM (polarizable continuum model) method can successfully be used to compute solvation free energies (ΔG_{solv}) with the appropriate the choice of cavity radii.[12] Likewise, the choice of cavity radii (the boundary between solute and solvent) is critical to determine solvation free energies (ΔG_{solv}) of dianions.[13] Many implicit solvation models such as the Born, PCM, and CPCM models have been applied to the calculation of solvation free energies (ΔG_{solv}) of dianions.[10f,j,14]

If the $B_nH_n^-$ intermediate is stable, the two-electron reduction process from B_nH_n may proceed with successive one-electron transfer pathways. The successive one-electron transfers versus a simultaneous two-electron transfer are governed by the ordering of reduction potentials for the first ($E°_1$) and second ($E°_2$) electron addition. The monoanion is unstable with respect to disproportionation to the neutral and dianion when $E°_1 - E°_2 < 0$ (potential inversion).[14a,15] However, disproportionation is controlled by solvation, and the

Received: December 9, 2011
Published: March 21, 2012

   dx.doi.org/10.1021/ic202660d | *Inorg. Chem.* 2012, 51, 4205−4214

Scheme 1. Thermodynamic Cycle Used to Calculate Reduction Potential of B_nH_n Species

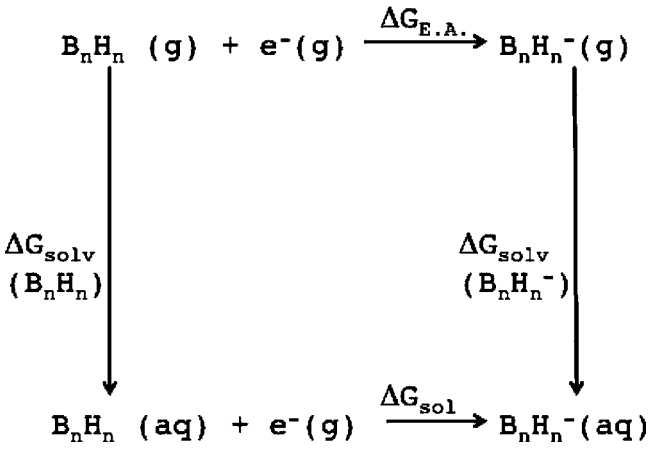

potential inversion is more often observed in solution rather than in the gas phase (eq 1).[10f,i,14a,15a,16]

$$2B_nH_n^- \rightarrow B_nH_n + B_nH_n^{2-} \quad (1)$$

When the difference of two reduction potentials is very small, the cyclic voltammetry produces a single voltammetric peak for two-electron transfer. About 98% of this potential compression is due to solvation, with a minor role from ion pairing.[15a,17] Barrière and Geiger[18] studied the two-electron transfer in $Ni(S_2C_2Fc_2)_2$ (Fc = $Fe(C_5H_5)(C_5H_4)$) which can occur either as successive one-electron transfers or as a single two-electron transfer depending on the medium. Consideration of the solvent effect is imperative to understand the multielectron transfer processes in solution.

The stability of the monoanion radical has been justified by electron delocalization.[14a,19] Mao et al.[20] reported that the extent of unpaired electron delocalization determines the solvent-dependent properties of paramagnetic organometallic complexes. In addition, several studies have shown[21] that the stability of mixed-valence ions toward disproportionation depends on solvent-induced electronic delocalization. However, electron localization in carotenoid di-ions can minimize Coulomb repulsion and enhance solvation stabilization, while electron delocalization reduces interaction with solvent.[15b] Thus, the rationalization of potential inversion in disproportionation reactions must consider the synergistic effect of solvent on the spin/charge delocalization in the monoanion radical.

Our ab initio computation with implicit solvation modeling will present the details of redox energetics (E°_{Red} versus standard hydrogen electrode (SHE)) of $B_nH_n^{0/-/2-}$ (n = 6−13) and $B_{12}X_{12}^{0/-/2-}$ (X = F, Cl, OH, and CH_3) boron clusters. Our E°_{Red} values will be compared to experimental oxidative stabilities ($E_{1/2}$) where $E^\circ_{red}(A) = E_{1/2}(B)$ in the reaction A + e^- → B. Our redox energetics include the free energy of disproportionation (ΔG_{dpro}, $2B_nH_n^- \rightarrow B_nH_n + B_nH_n^{2-}$) in aqueous solution and may provide insight into the electron transfer mechanism for polyborane-containing system. All experimental $E_{1/2}$ values and all calculated E°_{Red} values are relative to SHE in water.

COMPUTATIONAL DETAILS

The starting geometries of the boron clusters $B_nH_n^{0/-/2-}$ (n = 5−13) come from previous studies.[22] The B3LYP and M06-2X[23] exchange/correlation density functionals with the aug-cc-pvtz basis set were used to optimize geometries, compute vibrational frequencies, and calculate solvation free energies (ΔG_{solv}) (Scheme 1). We also applied the G4 level of theory[24] for $\Delta G_{E.A.}$ followed by calculation of ΔG_{solv} with B3LYP/aug-cc-pvtz and M06-2X/aug-cc-pvtz (G4/B3LYP and G4/M06-2X). Zero-point energies, thermal energies, and entropy corrections were computed in the gas phase using vibrational frequencies without scaling. For $\Delta G_{E.A.}$, we used adiabatic electron affinity calculations. The possibility of Jahn−Teller distortion and higher multiplicity electronic states of B_nH_n and $B_nH_n^-$ were considered and no electronic state issues were found (Supporting Information, Table S1). In the gas phase, the second electron binding energy (negative electron affinity) of small molecules is challenging to compute. Using a series of dielectric medium conditions (ε = 100, 10, 4, 2, and 1), Puiatti et al.[25] extrapolated the negative electron affinities. We also found that the directly calculated electron affinity of CO_3^- and SO_4^- monoanions in the gas phase (ε = 1) gave very similar results to the extrapolated value.[26] This nonadiabatic binding energy (negative electron affinity) provided reasonable lattice energies of M_2CO_3 and M_2SO_4 salts (M = Li^+, Na^+, and K^+).[26] We confirmed that the electron attachment of $B_6H_6^-$ in the gas phase also had a very similar value with the extrapolated result (Supporting Information, Figure S1).

Among the various implicit solvation models, the CPCM[27] with the UAKS cavity set[24] and the Pauling cavity set[24] were used in our study since water has a high dielectric constant (ε = 78.35). The SMD (solvation model density) method with the SMD cavity set was also used because it was developed for the "universal" application of solvation modeling including charged species.[28] The UAKS and Pauling cavity sets with the CPCM method investigate the sensitivity of solvation free energies to the cavity radii for anion and dianion species. The solvation free energies with the CPCM method include cavitation, dispersion, and repulsion energies (keyword = cav, dis, rep). The solvent excluded surface (keyword = surface = SES) is applied with average density integration point 10 $Å^{-2}$. The cavity surface is smoothed with the keyword "Addsph". We did not apply any specific keywords for the SMD solvation modeling. All calculations were carried out using the Gaussian09 package.[24]

The absolute value of the SHE has been debated to be between 4.11 and 4.52 V.[29] We used 4.28 V since the surface potential of water was considered.[29f,j] We note that the absolute potential of SHE in nonaqueous solution is different from that in water.[29g] A consideration of the "liquid junction potential" (LJP) and the correction for reference electrode are necessary when converting E°_{Red} in different solvent systems to water.[30] For example, the LJP of acetonitrile−water is 0.093 V.[1a,31] However, we did not apply the LJP since the reference electrode correction for acetonitrile has almost the same value as LJP but with opposite sign and thus the two almost cancel out.[10f] The widely used ion convention, IC (enthalpy of formation of the electron at nonzero temperatures is equal to the integrated heat capacity of the electron) is applied for the explicit electron in Scheme 1.[32] Electron attachment energetics in the gas phase ($\Delta G_{E.A.}$) and aqueous solution (ΔG_{sol}) in Scheme 1 can be summarized as follows (eq 2−4).

$$\Delta G_{sol} = \Delta G_{E.A.} + \Delta\Delta G_{solv} \quad (2)$$

$$\Delta G_{sol} = -nFE^o_{abs} \quad (3)$$

$$E^o_{red} = E^o_{abs} - 4.28 \quad (4)$$

The $\Delta\Delta G_{solv}$ is the difference in the free energy of solvation. The absolute reduction potential (E°_{abs}) is applied to the standard reduction potential (E°_{red}) with Faraday constant (F) and number of moles of electrons transferred per mol of reaction (n). All experimental oxidative stabilities ($E_{1/2}$) from the literature are converted to E°_{red} versus SHE unless explicitly indicated. We note that the smaller clusters B_nH_n (n = 6−9) are reported in water while the larger clusters B_nH_n (n = 10−12) are reported in acetonitrile.[1a] Some experimental oxidative stabilities ($E_{1/2}$) of $B_{12}X_{12}^{2-}$ (X = H, F, Cl)[33] are reported with the Fc/Fc^+ reference electrode, and we apply a 0.548 V correction to convert to SHE.[10f,29a,34]

dx.doi.org/10.1021/ic202660d | Inorg. Chem. 2012, 51, 4205−4214

RESULTS AND DISCUSSION

Electron Affinities of B_nH_n (n = 5−13) in the Gas Phase. The gas-phase electron attachment free energies ($\Delta G_{E.A.}$) of $B_nH_n^{0/-/2-}$ (n = 5−13) are presented in Figure 1

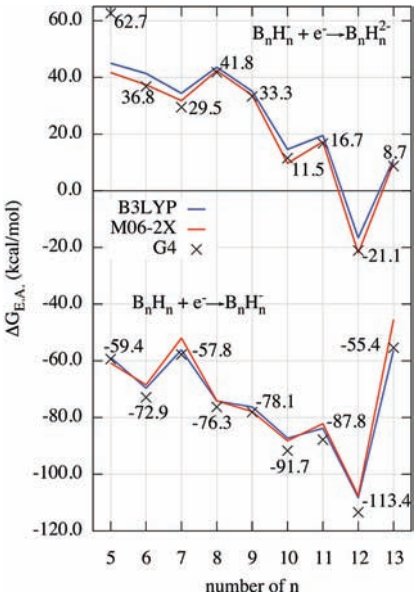

Figure 1. Electron attachment free energies ($\Delta G_{E.A.}$) of $B_nH_n^{0/-/2-}$ (n = 5−13) *hypercloso* boron clusters in gas phase obtained at the B3LYP/aug-cc-pvtz, M06-2X/aug-cc-pvtz, and G4 levels of theory. The values in the plot are the $\Delta G_{E.A.}$ from the G4 level of theory.

where $B_{12}H_{12}$ is the only species to give a bound second electron attachment ($B_{12}H_{12}^- + e^- \rightarrow B_{12}H_{12}^{2-}$, $\Delta G_{E.A.} < 0$). The trend of $\Delta G_{E.A.}$ in this study is similar to the reverse trend of adiabatic ionization potential for $B_nH_n^{2-} \rightarrow B_nH_n^- + e^-$ using B3LYP/6-311+G(d,p)//B3LYP/6-31G(d).[22a] Generally, the B3LYP functional gives similar attachment energies ($\Delta G_{E.A.}$) to the G4 level of theory for $B_nH_n + e^- \rightarrow B_nH_n^-$ while the M06-2X functional gives attachment energies ($\Delta G_{E.A.}$) similar to the G4 level of theory for $B_nH_n^- + e^- \rightarrow B_nH_n^{2-}$ (Figure 1 and Supporting Information, Table S3). For the first and second electron attachment free energies ($\Delta G_{E.A.}$), B3LYP and M06-2X functional results are both within 5.8 kcal/mol of the G4 results for B_nH_n (n = 6−13). The only exception is $B_{13}H_{13} + e^- \rightarrow B_{13}H_{13}^-$ with the M06-2X functional which differs by 9.9 kcal/mol from the G4 result (Supporting Information, Table S3). Pathak et al.[35] reported the electron affinity (EA) of $B_{12}H_{12}$ as 4.56 eV (105.1 kcal/mol) with B3LYP/6-311+G(d,p) while the EA of $B_{12}H_{12} + e^- \rightarrow B_{12}H_{12}^-$ in our study is between 4.69 eV (B3LYP/aug-cc-pvtz) and 4.92 eV (G4) (Figure 1 and Supporting Information, Table S3). $B_{10}H_{10}$, $B_{11}H_{11}$, and $B_{12}H_{12}$ are superhalogen species, which means the electron affinity is higher than the value of a halogen atom (3.0−3.6 eV, corresponding to 69.2−83.0 kcal/mol).[36] The second electron attachment energy of B_5H_5 by G4 level (62.7 kcal/mol) is quite different from the DFT (density functional theory) results (41.7 kcal/mol, M06-2X) while the first electron attachment energies are very similar among the three methods (Figure 1). For the B_5H_5 cluster, we used the cc-pvtz basis set rather than the aug-cc-pvtz basis set (i.e., no diffuse functions) because diffuse functions can cause artifacts for the unbound second electron of small dianions. Because of the large discrepancy of $\Delta G_{E.A.}$ by different methods and lack of literature data for reduction, we do not discuss B_5H_5 further (Figure 1). Cederbaum and co-workers discussed the nature of the second electron binding in $B_6H_6^{2-}$.[37] In contrast to $B_5H_5^- + e^- \rightarrow B_5H_5^{2-}$, DFT/aug-cc-pvtz and G4 show good agreement for $B_6H_6^- + e^- \rightarrow B_6H_6^{2-}$ (Figure 1). Electron attachment free energies of $B_nH_n^-$ ($B_nH_n^- + e^- \rightarrow B_nH_n^{2-}$, n = 5−13) become less positive as the size of the cluster increases (Figure 1). However, $\Delta G_{E.A.}$ of $B_7H_7^-$ is less positive than those of $B_8H_8^-$ and $B_9H_9^-$ while $\Delta G_{E.A.}$ of $B_{10}H_{10}^-$ is less positive than the $\Delta G_{E.A.}$ of $B_{11}H_{11}^-$ ($B_nH_n^- + e^- \rightarrow B_nH_n^{2-}$ in Figure 1). Both the size and the geometry of the cluster play a role in the electron attachment process (Table 1). If one normalizes the $\Delta G_{E.A.}$ by the cluster size, $B_{13}H_{13}$ neutral presents the smallest free energy gain ($\Delta G_{E.A.}/(BH)_n$) for the first electron attachment, which means the least favorable to electron attachment (Table 1).

Solvation Free Energies of B_nH_n (n = 5−13). The solvation free energies (ΔG_{solv}) of $B_nH_n^{0/-/2-}$ (n = 5−13) depend linearly on cluster size except for neutral $B_{13}H_{13}$, and the value of ΔG_{solv} greatly depends on the choice of cavity set (Figure 2). The CPCM/UAKS cavity set gives the smallest ΔG_{solv}, while the SMD method gives the largest ΔG_{solv}, and the CPCM/Pauling cavity set is between the two (Figure 2). The exception of $B_{13}H_{13}$ is due to much larger dipole moment (11.5 D with M06-2X(Pauling)) than all other dipole moments of B_nH_n (n = 6−12) (1.6, 4.2, 0.0, 0.0, 0.6, 2.2, and 4.2 D with M06-2X(Pauling), respectively). Because of its polar nature (a result of the electron description which has a contribution from $B_{12}H_{12}^{2-}$ with a capping BH^{2+} unit), $B_{13}H_{13}$ has a favorable solvation free energy in water. The SMD method for $B_{13}H_{13}$ gives ΔG_{solv} = −6.7 and −7.3 kcal/mol with B3LYP and M06-2X, respectively, while the CPCM/UAKS and CPCM/Pauling give positive values of ΔG_{solv} (Figure 2). The ΔG_{solv} of $B_nH_n^-$

Table 1. Free Energies of Electron Attachment per BH Unit ($\Delta G_{E.A.}/(BH)_n$ kcal/mol) of B_nH_n (n = 6−13) Boron Clusters[a]

	$B_nH_n(g) + e^-(g) \rightarrow B_nH_n^-(g)$			$B_nH_n^-(g) + e^-(g) \rightarrow B_nH_n^{2-}(g)$		
	B3LYP	M06-2X	G4/M06-2X	B3LYP	M06-2X	G4/M06-2X
B_6H_6	−11.6(−18.3)	−11.4(−18.4)	−12.1(−19.1)	6.9(−17.9)	6.2(−19.1)	6.1(−18.6)
B_7H_7	−8.0(−13.4)	−7.4(−13.0)	−8.3(−13.8)	4.9(−15.4)	4.5(−16.1)	4.2(−16.1)
B_8H_8	−9.3(−13.9)	−9.3(−14.0)	−9.5(−14.3)	5.4(−11.7)	5.3(−12.2)	5.2(−11.9)
B_9H_9	−8.5(−12.5)	−8.7(−12.9)	−8.7(−12.9)	3.9(−11.0)	3.7(−11.5)	3.7(−11.2)
$B_{10}H_{10}$	−8.7(−12.3)	−8.8(−12.6)	−9.2(−12.9)	1.5(−11.7)	1.0(−12.4)	1.1(−12.0)
$B_{11}H_{11}$	−7.6(−10.8)	−7.5(−10.8)	−8.0(−11.3)	1.8(−9.8)	1.6(−10.2)	1.5(−10.1)
$B_{12}H_{12}$	−9.0(−11.9)	−9.0(−11.9)	−9.5(−12.4)	−1.4(−12.0)	−1.8(−12.5)	−1.8(−12.3)
$B_{13}H_{13}$	−4.3(−5.9)	−3.3(−4.9)	−4.3(−5.9)	0.9(−8.5)	0.8(−8.7)	0.7(−8.7)

[a]The value in parentheses is $\Delta G_{sol}/(BH)_n$ with the CPCM/Pauling method.

dx.doi.org/10.1021/ic202660d | Inorg. Chem. 2012, 51, 4205−4214

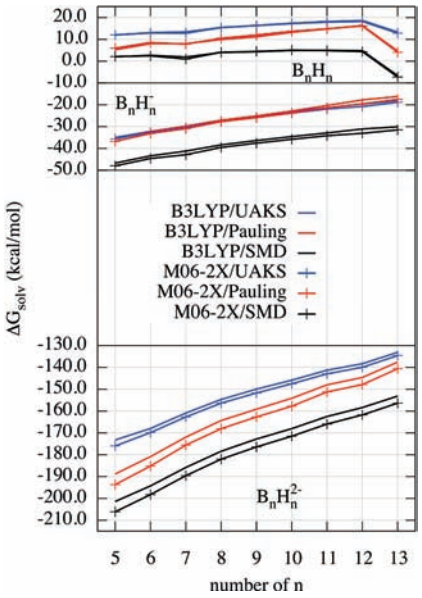

Figure 2. Solvation free energies (ΔG_{solv}) of B_nH_n, $B_nH_n^-$, and $B_nH_n^{2-}$ (n = 6–13) *hypercloso* boron clusters obtained with the CPCM/UAKS, CPCM/Pauling, and SMD solvation modeling.

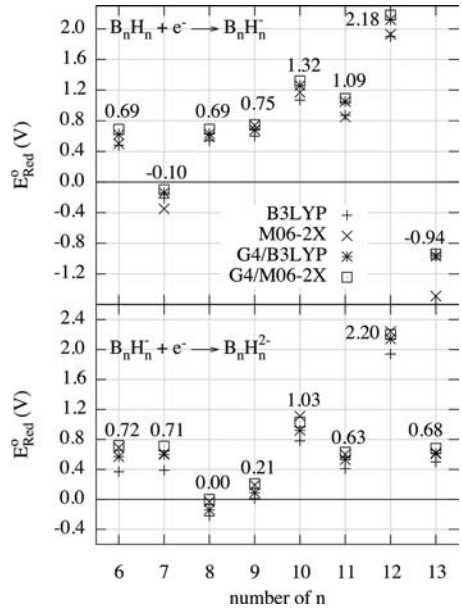

Figure 3. E°_{red} values of $B_nH_n^{0/-/2-}$ (n = 6–13) *hypercloso* boron clusters computed on the B3LYP/aug-cc-pvtz, M06-2X/aug-cc-pvtz, and G4 level of theory followed by CPCM/Pauling cavity set method. The values in plot are the E°_{red} from the G4/M06-2X(Pauling) method.

(n = 6–13) with CPCM/UAKS and CPCM/Pauling cavity sets are similar while ΔG_{solv} with the SMD method gives more negative ΔG_{solv} values by about 10 kcal/mol compared to CPCM results (Figure 2). For $B_nH_n^- + e^- \rightarrow B_nH_n^{2-}$ (n = 6–13), $\Delta G_{E.A.}$ values by DFT methods and by G4 level of theory agree within 5.0 kcal/mol (Figure 1 and Supporting Information, Table S3) while ΔG_{solv} values for dianions differ by more than 20 kcal/mol depending on the size of B_nH_n (n = 6–13) (Figure 2 and Supporting Information, Table S1). Thus, the solvation free energy differences ($\Delta\Delta G_{solv}$) between $B_nH_n^-$ and $B_nH_n^{2-}$ become significant factors in deciding the final E°_{Red} values (eq 2–4).

In a previous study of pK_{a2} values of diprotic acids ($HA^-(aq) \rightarrow H^+(aq) + A^{2-}(aq)$), the CPCM method with the Pauling cavity set gave better results than other cavity sets and also better than the SMD method (with SMD cavity set).[13] In addition, ΔG_{solv} of dianions with the CPCM/Pauling cavity set reproduced the dissolution free energies of alkali metal dianion salts (M_2X_1).[13,26] Therefore we decided to use the CPCM/Pauling combination to investigate the redox behavior of $B_nH_n^{0/-/2-}$ and the disproportionation of $B_nH_n^-$ (n = 6–13).

***E*°Red of B_nH_n (n = 6–13).** Figure 3 gives E°_{red} values for $B_nH_n^{0/-/2-}$ (n = 6–13) with the CPCM/Pauling cavity set method. The greatest variation in E°_{red} among the four methods (B3LYP, M06-2X, G4/B3LYP, G4/M06-2X) is 0.35 V (for $B_6H_6^- + e^- \rightarrow B_6H_6^{2-}$). However, the variation among the methods for all other boron clusters is less than 0.16 V except for $B_{13}H_{13}^{0/-}$ where the variation is 0.21 V (Figure 3). The larger variation of E°_{Red} among methods for $B_{13}H_{13}^{0/-}$ comes from the smaller $\Delta G_{E.A.}$ predicted by M06-2X relative to B3LYP and G4 (Supporting Information, Table S3). Klanberg and Muetterties[1c] reported the relative order of oxidative stability ($E_{1/2}$) as $B_9H_9^{2-} < B_{11}H_{11}^{2-} < B_{10}H_{10}^{2-} < B_{12}H_{12}^{2-}$ from polarographic studies. Our E°_{red} values for $B_nH_n^{0/-}$ and $B_nH_n^{-/2-}$ (n = 6–13) follow the same order of experimental oxidative stabilities (Figure 3). The $B_7H_7 + e^- \rightarrow B_7H_7^-$ is slightly nonspontaneous while $B_{13}H_{13} + e^- \rightarrow B_{13}H_{13}^-$ is quite nonspontaneous (E°_{Red}, −0.1 and −0.9 V respectively at G4/M06-2X(Pauling)) (Figure 3). Our E°_{Red} value for neutral $B_{13}H_{13}$ indicates that it is the least electron-accepting boron cluster in aqueous solution (Figure 3). It is interesting that the exceptional stability of $B_{13}H_{13}$ neutral in the gas phase has been noted previously.[22a] The $B_8H_8^- + e^- \rightarrow B_8H_8^{2-}$ is the only slightly nonspontaneous process for second electron attachments of B_nH_n (n = 6–13) (0.0 V at G4/M06-2X, Figure 3).

For $B_{12}H_{12}^- + e^- \rightarrow B_{12}H_{12}^{2-}$, our E°_{red} values are between 1.94 and 2.24 V while 1.67 V and >1.4 V of oxidative stability ($E_{1/2}$) have been reported (Figure 4).[2a,38] However, a recent cyclic voltammetry study suggests a value of 2.21 V in liquid SO_2.[33] The $E_{1/2}$ for $B_{10}H_{10}^{2-}$ (1.09 V) agrees well with our E°_{red} predictions (1.11 or 1.03 V, by M06-2X or G4/M06-2X, respectively, Figure 4 and Supporting Information, Table S4).[1a,38b] The polarographic study reported 0.29 V of $E_{1/2}$ for $B_{11}H_{11}^{2-}$ but the redox species was not well characterized.[1c,39] Later, a voltammetry study reported $E_{1/2}$ = 0.49 V for $B_{11}H_{11}^{2-}$.[1c,39] Indeed, our E°_{red} values are between 0.41 and 0.63 V. The $E_{1/2}$ of $B_9H_9^{2-}$ is 0.09 V while our E°_{red} values for $B_9H_9^{-/2-}$ are from 0.01 to 0.21 V.[1a,d] The oxidative stability ($E_{1/2}$) for the $B_9H_9^{2-}$ cluster is smaller than those of the boron clusters, $B_6H_6^{2-}$ and $B_8H_8^{2-}$. Indeed, the hydrolytic instability of $B_9H_9^{2-}$ has hindered the precise experimental determination of $E_{1/2}$.[40]

The polarographic study of the oxidative stability ($E_{1/2}$) of $B_6H_6^{2-}$ has yielded a value of −0.09 V.[1a,d] However, a more recent study[1e] reports a much larger value of 1.06 V in ethanol. Our predicted E°_{red} values for $B_6H_6^- + e^- \rightarrow B_6H_6^{2-}$ are between 0.37 and 0.72 V (Figure 4). The oxidative stability ($E_{1/2}$ = 1.06) of $B_6H_6^{2-}$ is slightly larger than that of $B_{10}H_{10}^{2-}$ ($E_{1/2}$ = 1.03, Figure 4). If we use ethanol as the solvent (rather than water) with the CPCM/Pauling cavity set, the E°_{Red} values for $B_6H_6^{-/2-}$ are reduced to 0.16 (B3LYP) and 0.49 V (G4/M06-2X). Thus, we suggest that the experimental $E_{1/2}$ value of −0.09 V is too small and the experimental value of 1.06 V is too large. Previous studies suggested the oxidative stability of

dx.doi.org/10.1021/ic202660d | *Inorg. Chem.* 2012, 51, 4205–4214

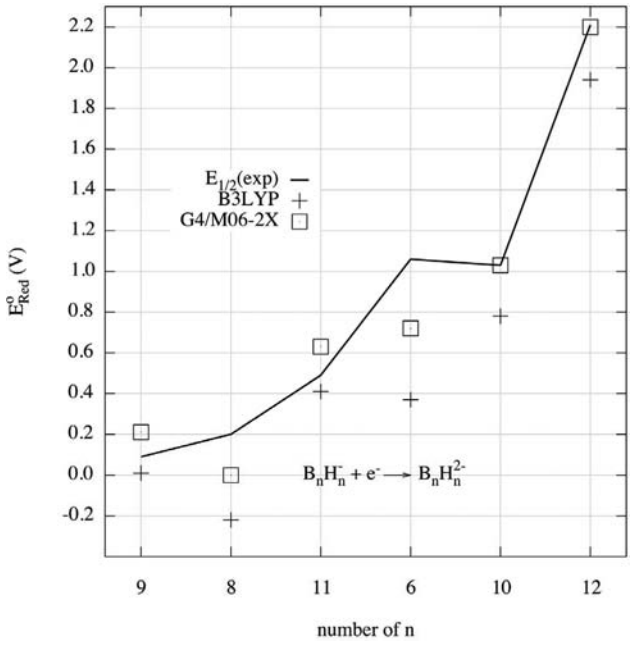

Figure 4. E°_{Red} values of $B_6H_6^{-/2-}$, $B_8H_8^{-/2-}$, $B_9H_9^{-/2-}$, $B_{10}H_{10}^{-/2-}$, $B_{11}H_{11}^{-/2-}$, and $B_{12}H_{12}^{-/2-}$ obtained on the G4/M06-2X(Pauling) and B3LYP(Pauling) method including experimental oxidative stability ($E_{1/2}$) of $B_nH_n^{2-}$.

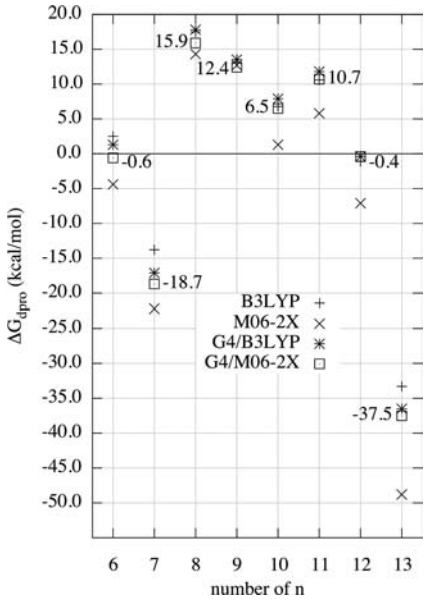

Figure 5. Disproportionation free energies (ΔG_{dpro}) of $B_nH_n^-$ (n = 6–13) *hypercloso* boron clusters computed on the B3LYP/aug-cc-pvtz, M06-2X/aug-cc-pvtz, and G4 levels of theory followed by the CPCM/Pauling cavity set method. The values in the plot are the ΔG_{dpro} from the G4/M06-2X method.

$B_7H_7^{-/2-}$ is smaller than that of $B_6H_6^{2-}$.[1a,b,d] Our computed E°_{red} value for $B_7H_7^{-/2-}$ (0.71 V, G4/M06-2X) is very similar to $B_6H_6^{2-}$ (0.72 V, G4/M06-2X, Figure 3 and Supporting Information, Table S4).

The difference between the E°_{red} of the neutral and monoanion boron hydride cluster is related to the stability toward disproportionation. The E°_{red} value of $B_7H_7 + e^- \rightarrow B_7H_7^-$ is the smallest for the first reductions of B_nH_n (n = 6–13) except $B_{13}H_{13}$ while $B_8H_8^- + e^- \rightarrow B_8H_8^{2-}$ gives the smallest E°_{red} value for the second reductions of B_nH_n (n = 6–13). The E°_{red} values of $B_7H_7^{0/-}$ show that the first reduction is more difficult than the second reduction (−0.10 − 0.71 V < 0.0, G4/M06-2X, Supporting Information, Table S4), which indicates potential inversion. However, Klanberg et al.[1d] reported that $B_7H_7^{2-}$ is the least stable dianion boron cluster and the most hydrolytically unstable. Except for $B_{13}H_{13}$, the E°_{Red} of $B_7H_7 + 2e^- \rightarrow B_7H_7^{2-}$ is the smallest of two electron attachments (0.31 V, G4/M06-2X, Supporting Information, Table S4). The computed E°_{Red} value (reduction potential of monoanion) of $B_8H_8^-$ is 0.00 V which compares to the experimental $E_{1/2}$ (oxidative stability of dianion) of 0.2 V (Figure 4).[1a,d] Since the calculated E°_{red} value of $B_8H_8 + e^- \rightarrow B_8H_8^-$ is 0.69 V (G4/M06-2X), B_8H_8 is predicted to have the normal ordering of potentials in aqueous solution (0.69–0.00 V > 0.0). The B3LYP functional generally underestimates the oxidative stability of $B_nH_n^{2-}$ relative to experiment and G4/M06-2X by more than 0.4 V (Figure 4). Indeed, it has been reported that B3LYP underestimates the experimental redox potential of transition metal complexes.[10c] However, reasonable E°_{Red} values (within 0.2 V of experiment) can be obtained when the G4/M06-2X method is applied (Figure 4 and Supporting Information, Table S4).

The disproportionation free energies (ΔG_{dpro}) of $2B_nH_n^- \rightarrow B_nH_n + B_nH_n^{2-}$ (n = 6–13) reveal the stability of monoanion radicals (Figure 5). For example, B_nH_n (n = 8–11) shows positive ΔG_{dpro} values with normal ordering of potential while B_nH_n (n = 7 and 13) gives negative ΔG_{dpro} values with potential inversion ($E^{\circ}_1 - E^{\circ}_2 < 0$ for reduction) (Figure 3 and Figure 5). The ΔG_{dpro} of B_6H_6 and $B_{12}H_{12}$ are borderline potential inversion cases (−0.6 and −0.4 kcal/mol, respectively, G4/M06-2X). Thus, a positive value of ΔG_{dpro} of B_nH_n indicates that the monoanion radical should be observed.

The M06-2X functional always gives the most negative ΔG_{dpro} values for every disproportionation of B_nH_n (n = 6–13) in this study (Figure 5). For example, the ΔG_{dpro} values for $B_{12}H_{12}^{2-}$ with B3LYP, G4/B3LYP, and G4/M06-2X are between −0.4 and −1.1 kcal/mol but the M06-2X functional result is much more negative (−7.1 kcal/mol). The variation of ΔG_{dpro} is within 2.5 kcal/mol for B_nH_n (n = 6–13) for all methods tested except for the M06-2X functional (Figure 5).

Since the geometric changes of B_nH_n (n = 6–13) *hypercloso* boron clusters are subtle during the reduction process and the solvation free energy (ΔG_{solv}) depends linearly on cluster size, the greatest effect on potential inversion comes from the electronic nature of $B_nH_n^-$ (n = 6–13) (Figure 2 and Supporting Information, Table S1). The best-known monanion radical is $B_8H_8^-$ where the fluxional nature is well established.[34b] This situation is different from other anions where fluxional behavior of the anion can induce potential inversion (i.e., $\Delta G_{dpro} < 0$).[41]

Speiser et al.[42] reported that the radical monoanion $B_8Cl_8^-$ is even more stable against disproportionation than $B_9Cl_9^-$. The stable $B_8H_8^-$, $B_{10}H_{10}^-$, $B_{11}H_{11}^-$, and $B_{12}H_{12}^-$ intermediates are used to explain the formation of reduction products in the literature. Our positive ΔG_{dpro} values by G4/M06-2X combination for $2B_nH_n^- \rightarrow B_nH_n + B_nH_n^{2-}$ (n = 8, 9, 10, 11) support the experimental observation of monoanion radicals (Figure 5).[1d,2d,43]

Many studies interpret the stability of monoanion radicals using delocalization of the unpaired electron.[1d,15b,19b,20,21b] The most stable monanion to disproportionation is $B_8H_8^-$ which shows strong electron delocalization in contrast to $B_{11}H_{11}^-$

dx.doi.org/10.1021/ic202660d | Inorg. Chem. 2012, 51, 4205–4214

(Figure 6). The monoanion radicals $B_7H_7^-$, $B_{12}H_{12}^-$, and $B_{13}H_{13}^-$ show a normal ordering of potential ($\Delta G_{dpro} < 0$)

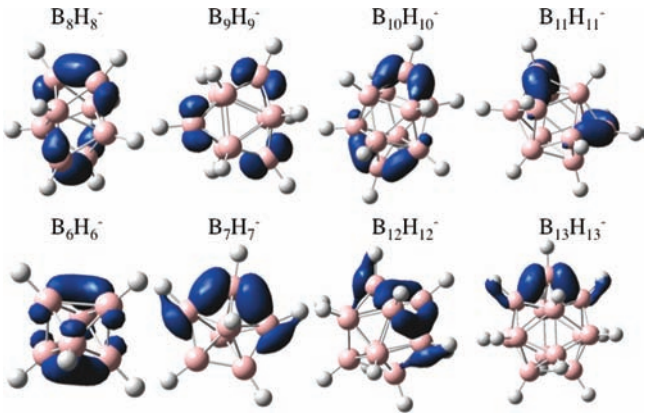

Figure 6. Spin densities of $B_nH_n^-$ (n = 6–13) boron clusters obtained from the M06-2X/aug-cc-pvtz level of theory (0.08 au isodensity).

which indicates that the monoanion radical should disproportionate to the neutral and dianion species (Figure 5). We interpret that the stability of $B_{11}H_{11}^-$ for disproportionation without electron delocalization comes from the smaller formation enthalpy (ΔH_f at 0 K, G4 level of theory) for $B_{11}H_{11}^{2-}$ (−4.6 kcal/mol) than those of $B_{10}H_{10}^{2-}$ (−5.6 kcal/mol) and $B_{12}H_{12}^{2-}$ (−77.8 kcal/mol) (Supporting Information, Table S8).

The free energy changes per BH unit $(\Delta G_{E.A.}/(BH)_n$ and $\Delta G_{sol}/(BH)_n)$ for $B_nH_n^{0/-}$ and $B_nH_n^{-/2-}$ (n = 6–13) are presented in Table 1. The stabilization by the first electron attachment of B_8H_8 in aqueous solution (−14.3 kcal/mol with G4/M06-2X) is more negative than those of B_nH_n (n = 9–13) but less negative than B_6H_6 (−19.1 kcal/mol, Table 1).

The values of E°_{Red} in solution and $\Delta G_{E.A.}$ in the gas phase for the first electron attachment ($B_nH_n + e^- \rightarrow B_nH_n^-$ (n = 6–12)) shows a linear relationship as found in the literature.[11a,c–h,15a] The value of E°_{Red} for $B_{13}H_{13}^{0/-}$ (−0.94 V, G4/M06–2X) is about 0.2 V less than a value expected from a linear relationship (−0.7 V, Figure 7). More favorable solvation of $B_{13}H_{13}$ than those of other neutral B_nH_n clusters induces this nonlinearity (Figure 2 and 7).

The correlation between E°_{Red} and $\Delta G_{E.A.}$ for the second electron attachment ($B_nH_n^- + e^- \rightarrow B_nH_n^{2-}$ (n = 6–12)) is given in Figure 8. Beyond the overall linear relationship, there are large deviations for several clusters, in particular $B_nH_n^-$ (n = 6 and 11). To understand the deviations, the decomposition of ΔG_{solv} (keyword = externaliteration) is useful. As noted previously, values of ΔG_{solv} for dianions are much larger than monoanions or neutral species so we limit our analysis to the dianions. As the size of the cluster increases, the contribution of hydrogen atoms (ΔG_{solv}(H)) to the total ΔG_{solv} of $B_nH_n^{2-}$ (n = 6–13) increases (Figure 9). The contribution of the non-electrostatic terms (cavity and dispersion energy, ΔG_{solv}(nonelec)) slowly increases as the size of cluster increases while the ΔG_{solv}(B) exponentially decreases as the exposure of boron atoms in $B_nH_n^{2-}$ to solvent decreases (Figure 9). The ΔG_{solv}(B) in $B_6H_6^{2-}$ (−44.6 kcal/mol) is more than two times ΔG_{solv}(B) in $B_7H_7^{2-}$ (−21.0 kcal/mol, Figure 9). This is caused by the significant increase in accessibility of boron atoms to solvent (Figure 9). For $B_nH_n^{2-}$ (n = 6–8), the ΔG_{solv}(B) contributes substantially to the total ΔG_{solv} of

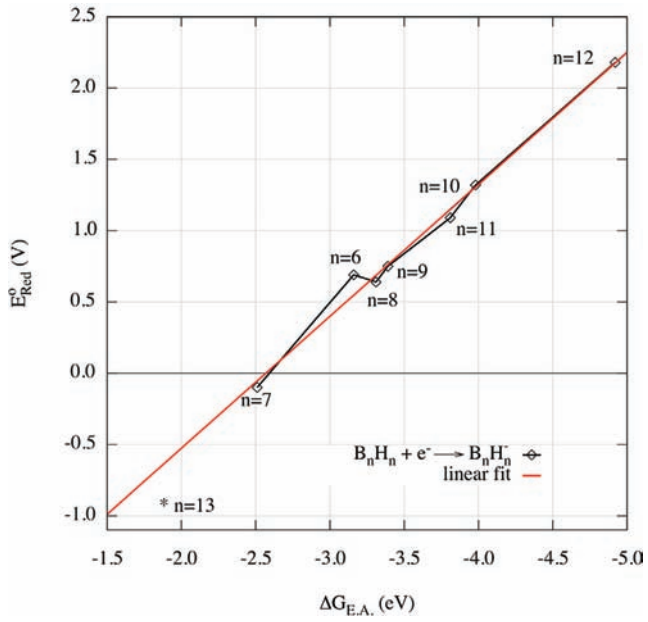

Figure 7. Correlation between gaseous electron attachment free energy ($\Delta G_{E.A.}$ by G4) and reduction potential (E°_{Red} by G4/M06-2X(Pauling)) in aqueous solution for $B_nH_n + e^- \rightarrow B_nH_n^-$.

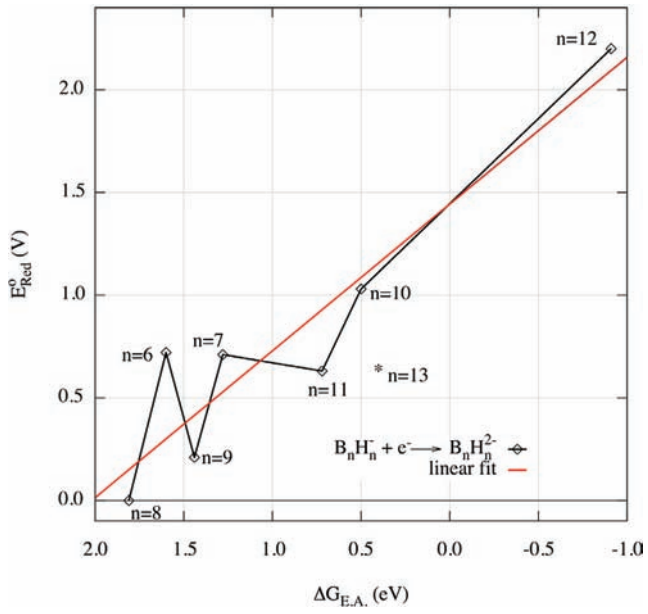

Figure 8. Correlation between gaseous electron attachment free energy ($\Delta G_{E.A.}$ by G4) and reduction potential (E°_{Red} by G4/M06-2X(Pauling)) in aqueous solution for $B_nH_n^- + e^- \rightarrow B_nH_n^{2-}$.

dianion while ΔG_{solv}(B) of $B_nH_n^{2-}$ (n = 9–13) is relatively negligible. The deviation of $B_{11}H_{11}^{2-}$ from linearity (Figure 9) is due to the ΔG_{solv}(H) of the hydrogen attached to the seven-coordinate boron atom in $B_{11}H_{11}^{2-}$ which is about 3 kcal/mol less than ΔG_{solv}(H) from other hydrogen atoms (Supporting Information, Table S7). The smaller ΔG_{solv} of the dianion leads to a smaller E°_{Red} value than expected (Figure 8).

***E*°Red of $B_{12}X_{12}$ (X = H, F, Cl, OH, and CH_3).** The experimental redox chemistry of the persubstituted dodecaborates $B_{12}X_{12}$ has been reported.[1a,5,9a,c,g,33,44] The E°_{Red} of $B_{12}X_{12}^{-/2-}$ (X = H, F, Cl, OH, and CH_3, Table 2) is in the order $B_{12}Cl_{12}^{2-}$ > $B_{12}F_{12}^{2-}$ > $B_{12}H_{12}^{2-}$ > $B_{12}(CH_3)_{12}^{2-}$ >

dx.doi.org/10.1021/ic202660d | Inorg. Chem. 2012, 51, 4205–4214

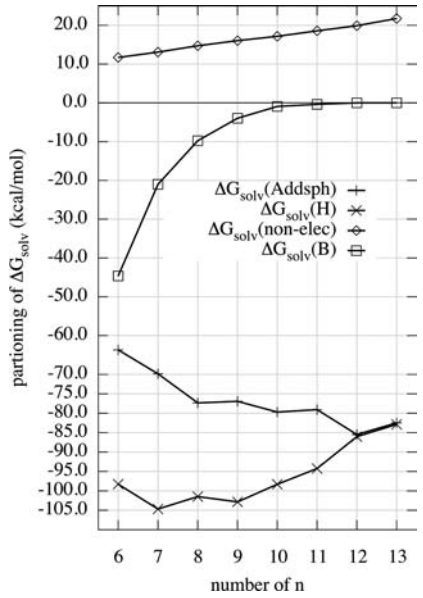

Figure 9. Partitioning of solvation free energies (ΔG_{solv}) of $B_nH_n^{2-}$ (n = 6−13) boron clusters obtained from the M06-2X/Pauling cavity set method (keyword = externaliteration) (ΔG_{solv}(B) = solvation free energy by all boron atoms, ΔG_{solv}(H) = solvation free energy by all hydrogen atoms, ΔG_{solv}(nonelec) = solvation free energy by dispersion and cavitation, and ΔG_{solv}(Addsph) = solvation free energy by smoothed surface for the cavity volume).

$B_{12}(OH)_{12}^{2-}$ with B3LYP and M06-2X functional (G4/M06-2X calculations could not be carried out for X≠H). Ivanov et al.[9a] reported about 1.9−2.0 V for the oxidative stability ($E_{1/2}$) of $B_{12}F_{12}^{2-}$ in ethylene carbonate:dimethyl carbonate (50:50 in volume) solution and suggested the salts of the radical monoanion $B_{12}F_{12}^{-}$ might be isolable. Our positive ΔG_{dpro} for $2B_{12}F_{12}^{-} \rightarrow B_{12}F_{12} + B_{12}F_{12}^{2-}$ (14.4 kcal/mol, M06-2X) supports the possibility of $B_{12}F_{12}^{-}$ isolation (Table 3). However, a more recent study of $B_{12}X_{12}^{2-}$ (X = H, F, Cl, Br, and I) in liquid SO_2 solution gives an oxidative stability of 2.3 V for $B_{12}F_{12}^{2-}$, which is similar to the result with the M06-2X functional (Table 2).[33] The oxidative stability ($E_{1/2}$) of $B_{12}(CH_3)_{12}^{2-}$ has been reported as 0.44 V (and corrected to SHE as 0.6 V)[9c,45] which can be compared to 0.39 V (B3LYP) or 0.67 V (M06-2X) (Table 2). The value of ΔG_{dpro} (18.9 kcal/mol) with the M06-2X functional supports the well-known stability of the $B_{12}(CH_3)_{12}^{-}$ monoanion radical (Table 3).[9c]

Table 3. Disproportionation Free Energies in Gas[a] with DFT Functionals (B3LYP and M06-2X) and in Aqueous Solution[b] of $B_{12}X_{12}$ (X = H, F, Cl, OH, and CH_3) *hypercloso* Boron Clusters with CPCM(Pauling) Solvation Modeling

$B_{12}X_{12}$	ΔG_{gas}[c] B3LYP	ΔG_{gas}[c] M06-2X	ΔG_{dpro} B3LYP	ΔG_{dpro} M06-2X
$B_{12}H_{12}$	91.7	85.7	−1.1	−7.1
$B_{12}F_{12}$	97.9	99.1	14.0	14.4
$B_{12}Cl_{12}$	77.6	78.6	8.8	10.0
$B_{12}(OH)_{12}$	84.4	89.0	9.2	13.2
$B_{12}(CH_3)_{12}$	90.5	83.3	26.1	18.9

[a] ΔG_{gas}, $2B_nX_n^{-}(g) \rightarrow B_nX_n(g) + B_nX_n^{2-}(g)$. [b] ΔG_{dpro}, $2B_{12}X_{12}^{-}(aq) \rightarrow B_{12}X_{12}(aq) + B_{12}X_{12}^{2-}(aq)$. [c] G4 level of theory is not applied because of the computational expense.

The reported oxidative stability ($E_{1/2}$) of $B_{12}Cl_{12}^{2-}$, (2.34 V, corrected to SHE as 2.6 V), can be compared to our E°_{Red} values of 2.54/2.98 V for $B_{12}Cl_{12}^{-/2-}$(B3LYP/M06-2X, Table 2).[1a,44] A recent cyclic voltammetry study in liquid SO_2 solution reported 2.15 V with the ferrocene/ferrocenium reference electrode (and corrected to SHE as 2.70 V), which is between B3LYP and M06-2X functional results (Table 2).[33] The first one-electron reduction E°_{Red} value from the neutral $B_{12}Cl_{12} + e^{-} \rightarrow B_{12}Cl_{12}^{-}$ with the B3LYP and M06-2X functional gives 2.92 and 3.41 V, respectively, which can be compared to (corrected) the cyclic voltammetry value of 3.1 V (Table 2).[33] The identification of $B_{12}Cl_{12}$ was done by NMR and UV/vis spectra.[33,46] The E°_{Red} values of $B_{12}X_{12}$ (X = H, F, Cl, and CH_3) are between 1.20 and 3.41 V by M06-2X functional (Table 2).

Table 2. E°_{red} Values of $B_{12}X_{12}^{0/-/2-}$ (X = H, F, Cl, OH, and CH_3) Boron Clusters with the DFT/CPCM(Pauling) Method

reduction (E°_{Red}, V)	B3LYP[a]	M06-2X[a]	$E_{1/2}$ (V)	σ_p[c]
$B_{12}(OH)_{12} + e^{-} \rightarrow B_{12}(OH)_{12}^{-}$	0.79(−79.3)	1.20(−88.0)		−0.37
$B_{12}(CH_3)_{12} + e^{-} \rightarrow B_{12}(CH_3)_{12}^{-}$	1.52(−101.5)	1.80(−107.6)		−0.17
$B_{12}H_{12} + e^{-} \rightarrow B_{12}H_{12}^{-}$	1.93(−108.3)	2.12(−107.6)		0.00
$B_{12}F_{12} + e^{-} \rightarrow B_{12}F_{12}^{-}$	2.64(−129.6)	3.09(−139.2)		0.06
$B_{12}Cl_{12} + e^{-} \rightarrow B_{12}Cl_{12}^{-}$	2.92(−135.5)	3.41(−146.0)	(about 3.1)[b]	0.23
$B_{12}(OH)_{12}^{-} + e^{-} \rightarrow B_{12}(OH)_{12}^{2-}$	0.39(5.1)	0.63(1.0)	1.3	−0.37
$B_{12}(CH_3)_{12}^{-} + e^{-} \rightarrow B_{12}(CH_3)_{12}^{2-}$	0.39(−11.0)	0.98(−24.3)	0.6	−0.17
$B_{12}H_{12}^{-} + e^{-} \rightarrow B_{12}H_{12}^{2-}$	2.24(−16.6)	2.14(−22.0)	1.7(2.2)[b]	0.00
$B_{12}F_{12}^{-} + e^{-} \rightarrow B_{12}F_{12}^{2-}$	2.03(−31.7)	2.47(−40.1)	2.0(2.3)[b]	0.06
$B_{12}Cl_{12}^{-} + e^{-} \rightarrow B_{12}Cl_{12}^{2-}$	2.54(−57.9)	2.98(−67.3)	2.6(2.7)[b]	0.23
$B_{12}(OH)_{12} + 2e^{-} \rightarrow B_{12}(OH)_{12}^{2-}$	0.59(−74.2)	0.92(−87.0)		−0.37
$B_{12}(CH_3)_{12} + 2e^{-} \rightarrow B_{12}(CH_3)_{12}^{2-}$	0.96(−112.5)	1.40(−131.9)		−0.17
$B_{12}H_{12} + 2e^{-} \rightarrow B_{12}H_{12}^{2-}$	2.09(−124.9)	2.13(−129.6)		0.00
$B_{12}F_{12} + 2e^{-} \rightarrow B_{12}F_{12}^{2-}$	2.34(−161.3)	2.78(−179.3)		0.06
$B_{12}Cl_{12} + 2e^{-} \rightarrow B_{12}Cl_{12}^{2-}$	2.73(−193.4)	3.20(−213.3)		0.23

[a] The $\Delta G_{E.A.}$ and ΔG_{solv} of $B_{12}X_{12}^{0/-/2-}$ are calculated with B3LYP and M06-2X functional. The value in parentheses is $\Delta G_{E.A.}$ obtained with DFT functionals. Because of the computational expense, G4 level of theory is not applied to $B_{12}X_{12}$ systems. [b] The value in parentheses is obtained from the measurement in liquid SO_2 solution, see ref 41. [c] The Hammett σ_p parameter comes from March, J. *Advanced Organic Chemsitry*; John & Wiley: New York, 1985.

dx.doi.org/10.1021/ic202660d | *Inorg. Chem.* 2012, 51, 4205−4214

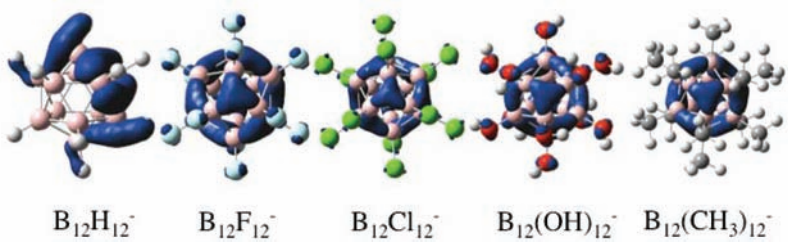

Figure 10. Spin densities of $B_{12}X_{12}^-$ (X = H, F, Cl, OH, and CH_3) *hypercloso* boron clusters obtained on the M06-2X/aug-cc-pvtz level of theory (0.04 au isodensity).

Knoth et al.[38b] reported the oxidative stability decreased whenever the hydroxyl group replaced the hydride of $B_{12}H_{12}^{2-}$. Recently, Van et al.[9f] reported the value of $E_{1/2}$ as 0.45 V for $B_{12}(OH)_{12}^{2-}$ in CH_3CN and 0.75 V in water versus the ferrocenium/ferrocene reference electrode couple (1.00 V in CH_3CN and 1.30 V in water versus SHE[47]). Our E°_{Red} values of $B_{12}(OH)_{12}^{-/2-}$ in water (using any cavity set) are much smaller than 1.00 V (Supporting Information, Table S4). The largest calculated E°_{Red} value of $B_{12}(OH)_{12}^{-/2-}$ (0.63 V) comes from the M06-2X functional which is 0.67 V smaller than the experimental value (1.30 V in water versus SHE, Table 2). All of the other experimental oxidative stabilities ($E_{1/2}$) are between B3LYP and M06-2X functional results (Table 2). Therefore, we recommend a redetermination of $E_{1/2}$ for $B_{12}(OH)_{12}^{2-}$.

McKee[22b] reported that the order of Hammett (σ_p) parameter for $B_{12}X_{12}^{2-}$ agreed with the order of gaseous stability for $B_{12}H_{12}^{n-} + 12HX \rightarrow B_{12}X_{12}^{n-} + 12H_2$ (n = 0, 1, 2; X = H, F, OH, and CH_3), $B_{12}F_{12}^{2-} > B_{12}H_{12}^{2-} > B_{12}(CH_3)_{12}^{2-} > B_{12}(OH)_{12}^{2-}$. The trend of E°_{Red} value in this study also agrees well with the order of the Hammett (σ_p) parameter (Table 2). The positive ΔG_{dpro} of $B_{12}X_{12}^-$ (X = F, Cl, OH, and CH_3) in our study supports the stability of monoanion radical $B_{12}X_{12}^-$ (X = F, Cl, OH, and CH_3) in experiment (Table 3).[9a−c,f,33,44,46] The unpaired spin density of $B_{12}X_{12}^-$ (X = F, Cl, OH, and CH_3) shows strong delocalization which is like that of $B_{12}H_{12}^-$ (Figure 6 and Figure 9). The unpaired electron tends to locate on the boron atoms of the cluster rather than on the functional groups of $B_{12}X_{12}^-$ (X = F, Cl, OH, and CH_3), in agreement with the observations from previous studies (Figure 10).[9c,f,33]

CONCLUSIONS

The reduction potentials (E°_{Red}) of *hypercloso* boron hydrides B_nH_n (n = 6−13) and persubstituted dodecaboron hydrides $B_{12}X_{12}$ (X = F, Cl, OH, and CH_3) have been studied by G4 level of theory and DFT methods with implicit solvation modeling. The E°_{Red} with G4/M06-2X provides the best agreement with experimental oxidative stability ($E_{1/2}$) of $B_nH_n^{2-}$ (n = 6−12). The experimental oxidative stability ($E_{1/2}$) of $B_{12}X_{12}^{2-}$ (X = F, Cl, OH, and CH_3) is usually located between the B3LYP and M06-2X values of E°_{Red}. Our oxidative stabilities of $B_6H_6^{2-}$ and $B_{12}(OH)_{12}^{2-}$ deviate more than expected from the experimental values and we suggest that more experiments may be needed. The B3LYP functional tends to underestimate E°_{Red} values while the M06-2X functional tends to overestimate E°_{Red} values. The ΔG_{solv} depends greatly on the choice of the cavity radii set while the dependence on density functional is modest. The CPCM/UAKS cavity set gives the smallest ΔG_{solv} and the SMD method gives the largest ΔG_{solv} of $B_nH_n^{0/-/2-}$ (n = 6−13). The stability of monoanion radicals of B_nH_n (n = 6−13) to disproportionation ($2B_nH_n^- \rightarrow B_nH_n + B_nH_n^{2-}$) decreases in the order $B_8H_8^- > B_9H_9^- > B_{11}H_{11}^- > B_{10}H_{10}^-$ while $B_7H_7^-$ and $B_{13}H_{13}^-$ give very spontaneous disproportionation because of potential inversion. The delocalization of spin density in the $B_nH_n^-$ radical anions explains their stability but $B_{11}H_{11}^-$ gives a positive ΔG_{dpro} without distinct delocalization of spin density. A good correlation between $\Delta G_{E.A.}$ and E°_{Red} is established for the first electron attachments of B_nH_n (n = 6−13) but the correlation for second electron attachments of B_nH_n (n = 6−13) deviates from a linear relationship in the case of B_6H_6, $B_{11}H_{11}$, and $B_{13}H_{13}$. The solvation free energy differences ($\Delta\Delta G_{solv}$) between $B_nH_n^-$ and $B_nH_n^{2-}$ are significant factors in determining E°_{Red} or $E_{1/2}$ in aqueous solution. The partitioning of solvation free energies reveals why the correlation between $\Delta G_{E.A.}$ and E°_{Red} for $B_nH_n^{-/2-}$ (n = 6, 7, and 11) deviates from general a linear relationship.

ASSOCIATED CONTENT

Supporting Information

Thermodynamic values are given for $B_nH_n^{0/-/2-}$ and $B_{12}X_{12}^{0/-/2-}$ (n = 5−13 and X = F, Cl, OH, and CH_3) in Table S1. Table S2 presents the electronic energies, enthalpies, and free energies of $B_nH_n^{0/-/2-}$ at the G4 level of theory. Table S3 presents the free energies of electron attachment ($\Delta G_{E.A.}$). The E°_{Red} values with different DFT functionals and cavity sets are summarized in Table S4. The disproportionation free energies (ΔG_{dpro}) with the UAKS, Pauling, and SMD cavity sets are presented in Table S5. Table S6 summarizes the solvation free energy differences ($\Delta\Delta G_{solv}$) of $B_nH_n^{0/-}$ and $B_nH_n^{-/2-}$. Table S7 presents the partitioning of solvation free energies (ΔG_{solv}) for $B_nH_n^{2-}$ (n = 6−12) with the M06-2X(Pauling). Table S8 gives heat of formation (ΔH_f at 0K) of $B_nH_n^{0/-/2-}$ (n = 5−13) at the G4 level of theory. The geometries of $B_nH_n^{0/-/2-}$ (n = 5−13) and $B_nX_n^{0/-/2-}$ (X = F, Cl, OH, and CH_3) with the B3LYP functional are presented in Table S9. Figure S1 presents the electron affinity of $B_6H_6^-$ in a series of dielectric media. This material is available free of charge via the Internet at http://pubs.acs.org.

AUTHOR INFORMATION

Corresponding Author

*E-mail: mckee@chem.auburn.edu.

Notes

The authors declare no competing financial interest.

ACKNOWLEDGMENTS

Computer time was made available on the Alabama Supercomputer Network. The authors thank Dr. D. Stanbury and Dr. V. Cammarata for helpful discussions.

REFERENCES

(1) (a) Morris, J. H.; Gysling, H. J.; Reed, D. *Chem. Rev.* **1985**, *85*, 51−76. (b) Muetterties, E. L.; Balthis, J. H.; Chia, Y. T.; Knoth, W. H.; Miller, H. C. *Inorg. Chem.* **1964**, *3*, 444−451. (c) Klanberg, F.; Muetterties, E. L. *Inorg. Chem.* **1966**, *5*, 1955−1960. (d) Klanberg, F.; Eaton, D. R.; Guggenberger, L. J.; Muetterties, E. L. *Inorg. Chem.* **1967**, *6*, 1271−1281. (e) Preetz, W.; Peters, G. *Eur. J. Inorg. Chem.* **1999**, 1831−1846. (f) Muetterties, E. L.; Knoth, W. H. *Polyhedral Boranes*; Marcel Dekker Inc.: New York, 1968.

(2) (a) Wiersema, R. J.; Middaugh, R. L. *Inorg. Chem.* **1969**, *8*, 2074−2079. (b) Watson-Clark, R. A.; Hawthorne, M. F. *Inorg. Chem.* **1997**, *36*, 5419−5420. (c) Volkov, O.; Hu, C. H.; Kolle, U.; Paetzold, P. *Z. Anorg. Allg. Chem.* **2005**, *631*, 1909−1911. (d) Volkov, O.; Paetzold, P.; Hu, C. H. *Z. Anorg. Allg. Chem.* **2006**, *632*, 945−948. (e) Zhizhin, K. Y.; Zhdanov, A. P.; Kuznetsov, N. T. *Russ. J. Inorg. Chem.* **2010**, *55*, 2089−2127.

(3) (a) Hawthorn, M. F.; Pilling, R. L.; Stokely, P. F. *J. Am. Chem. Soc.* **1965**, *87*, 1893−1899. (b) Hawthorne, M. F.; Pilling, R. L.; Stokely, P. F.; Garrett, P. M. *J. Am. Chem. Soc.* **1963**, *85*, 3704−3705. (c) Chamberland, B. L.; Muetterties, E. L. *Inorg. Chem.* **1964**, *3*, 1450−1456. (d) Wiersema, R. J.; Middaugh, R. L. *Inorg. Chem.* **1969**, *8*, 2074−2079.

(4) Kaczmarc., A.; Kolski, G. B.; Townsend, W. P. *J. Am. Chem. Soc.* **1965**, *87*, 1413−1413.

(5) Avelar, A.; Tham, F. S.; Reed, C. A. *Angew. Chem., Int. Ed.* **2009**, *48*, 3491−3493.

(6) (a) Geis, V.; Guttsche, K.; Knapp, C.; Scherer, H.; Uzun, R. *Dalton Trans.* **2009**, 2687−2694. (b) Ivanov, S. V.; Davis, J. A.; Miller, S. M.; Anderson, O. P.; Strauss, S. H. *Inorg. Chem.* **2003**, *42*, 4489−4491. (c) Ivanov, S. V.; Lupinetti, A. J.; Solntsev, K. A.; Strauss, S. H. *J. Fluor. Chem.* **1998**, *89*, 65−72. (d) Peryshkov, D. V.; Popov, A. A.; Strauss, S. H. *J. Am. Chem. Soc.* **2009**, *131*, 18393−18403.

(7) Jelen, F.; Olejniczak, A. B.; Kourilova, A.; Lesnikowski, Z. J.; Palecek, E. *Anal. Chem.* **2008**, *81*, 840−844.

(8) Jalisatgi, S. S.; Kulkarni, V. S.; Tang, B.; Houston, Z. H.; Lee, M. W.; Hawthorne, M. F. *J. Am. Chem. Soc.* **2011**, *133*, 12382−12385.

(9) (a) Ivanov, S. V.; Miller, S. M.; Anderson, O. P.; Solntsev, K. A.; Strauss, S. H. *J. Am. Chem. Soc.* **2003**, *125*, 4694−4695. (b) Warneke, J.; Dulcks, T.; Knapp, C.; Gabel, D. *Phys. Chem. Chem. Phys.* **2011**, *13*, 5712−5721. (c) Peymann, T.; Knobler, C. B.; Hawthorne, M. F. *Chem. Commun.* **1999**, 2039−2040. (d) Peymann, T.; Knobler, C. B.; Khan, S. I.; Hawthorne, M. F. *J. Am. Chem. Soc.* **2001**, *123*, 2182−2185. (e) Maderna, A.; Knobler, C. B.; Hawthorne, M. F. *Angew. Chem., Int. Ed.* **2001**, *40*, 1661−1664. (f) Van, N.; Tiritiris, I.; Winter, R. F.; Sarkar, B.; Singh, P.; Duboc, C.; Muñoz-Castro, A.; Arratia-Pérez, R.; Kaim, W.; Schleid, T. *Chem.—Eur. J.* **2010**, *16*, 11242−11245. (g) Lee, M. W.; Farha, O. K.; Hawthorne, M. F.; Hansch, C. H. *Angew. Chem., Int. Ed.* **2007**, *46*, 3018−3022.

(10) (a) Baik, M. H.; Friesner, R. A. *J. Phys. Chem. A* **2002**, *106*, 7407−7412. (b) Dutton, A. S.; Fukuto, J. M.; Houk, K. N. *Inorg. Chem.* **2005**, *44*, 4024−4028. (c) Roy, L. E.; Jakubikova, E.; Guthrie, M. G.; Batista, E. R. *J. Phys. Chem. A* **2009**, *113*, 6745−6750. (d) Si, D.; Li, H. *J. Phys. Chem. A* **2009**, *113*, 12979−12987. (e) Namazian, M.; Lin, C. Y.; Coote, M. L. *J. Chem. Theory Comput.* **2010**, *6*, 2721−2725. (f) Lord, R. L.; Schultz, F. A.; Baik, M. H. *Inorg. Chem.* **2010**, *49*, 4611−4619. (g) Fry, A. J.; Davis, A. P. *J. Phys. Chem. A* **2010**, *114*, 12299−12304. (h) Gennaro, A.; Isse, A. A.; Lin, C. Y.; Coote, M. L. *J. Phys. Chem. B.* **2011**, *115*, 678−684. (i) Jiao, D.; Leung, K.; Rempe, S. B.; Nenoff, T. M. *J. Chem. Theory Comput.* **2010**, *7*, 485−495. (j) Surawatanawong, P.; Tye, J. W.; Darensbourg, M. Y.; Hall, M. B. *Dalton Trans.* **2010**, *39*, 3093−3104. (k) Blumberger, J.; Tateyama, Y.; Sprik, M. *Comput. Phys. Commun.* **2005**, *169*, 256−261. (l) Vande-Vondele, J.; Sulpizi, M.; Sprik, M. *Angew. Chem., Int. Ed.* **2006**, *45*, 1936−1938. (m) VandeVondele, J.; Ayala, R.; Sulpizi, M.; Sprik, M. *J. Electroanal. Chem.* **2007**, *607*, 113−120. (n) Costanzo, F.; Sulpizi, M.; Guido Della Valle, R.; Sprik, M. *J. Chem. Theory Comput.* **2008**, *4*, 1049−1056. (o) Cheng, J.; Sulpizi, M.; Sprik, M. *J. Chem. Phys.* **2009**, *131*, 154504−154520.

(11) (a) Parker, V. D. *J. Am. Chem. Soc.* **1976**, *98*, 98−103. (b) Ballard, R. E. *Chem. Phys. Lett.* **1976**, *42*, 97−98. (c) Ruoff, R. S.; Kadish, K. M.; Boulas, P.; Chen, E. C. M. *J. Phys. Chem.* **1995**, *99*, 8843−8850. (d) Lobach, A. S.; Strelets, V. V. *Russ. Chem. Bull.* **2001**, *50*, 1593−1595. (e) Kebarle, P.; Chowdhury, S. *Chem. Rev.* **1987**, *87*, 513−534. (f) Shalev, H.; Evans, D. H. *J. Am. Chem. Soc.* **1989**, *111*, 2667−2674. (g) Nelsen, S. F.; Teasley, M. F.; Bloodworth, A. J.; Eggelte, H. J. *J. Org. Chem.* **1985**, *50*, 3299−3302. (h) Betowski, L. D.; Enlow, M.; Riddick, L.; Aue, D. H. *J. Phys. Chem. A* **2006**, *110*, 12927−12946.

(12) (a) Sadlej-Sosnowska, N. *Theor. Chem. Acc.* **2007**, *118*, 281−293. (b) Ho, J.; Coote, M. L. *J. Chem. Theory Comput.* **2009**, *5*, 295−306. (c) Chipman, D. M. *J. Phys. Chem. A* **2002**, *106*, 7413−7422. (d) Camaioni, D. M.; Dupuis, M.; Bentley, J. *J. Phys. Chem. A* **2003**, *107*, 5778−5788. (e) Ginovska, B.; Camaioni, D. M.; Dupuis, M.; Schwerdtfeger, C. A.; Gil, Q. *J. Phys. Chem. A* **2008**, *112*, 10604−10613. (f) Alexeev, Y.; Windus, T. L.; Zhan, C.-G.; Dixon, D. A. *I. J. Quant. Chem.* **2005**, *102*, 775−784. (g) Gutowski, K. E.; Dixon, D. A. *J. Phys. Chem. A* **2006**, *110*, 8840−8856.

(13) Lee, T. B.; McKee, M. L. *Phys. Chem. Chem. Phys.* **2011**, *13*, 10258−10269.

(14) (a) Evans, D. H.; Hu, K. *J. Chem. Soc., Faraday Trans.* **1996**, *92*, 3983−3990. (b) Felton, G. A. N.; Vannucci, A. K.; Chen, J.; Lockett, L. T.; Okumura, N.; Petro, B. J.; Zakai, U. I.; Evans, D. H.; Glass, R. S.; Lichtenberger, D. L. *J. Am. Chem. Soc.* **2007**, *129*, 12521−12530. (c) Muratsugu, S.; Sodeyama, K.; Kitamura, F.; Sugimoto, M.; Tsuneyuki, S.; Miyashita, S.; Kato, T.; Nishihara, H. *J. Am. Chem. Soc.* **2009**, *131*, 1388−1389.

(15) (a) Evans, D. H. *Chem. Rev.* **2008**, *108*, 2113−2144. (b) Hapiot, P.; Kispert, L. D.; Konovalov, V. V.; Savéant, J.-M. *J. Am. Chem. Soc.* **2001**, *123*, 6669−6677. (c) Gileadi, E. *J. Electroanal. Chem.* **2002**, *532*, 181−189.

(16) (a) Hush, N. S.; Blackledge, J. *J. Chem. Phys.* **1955**, *23*, 514−517. (b) Fry, A. J. *Tetrahedron* **2006**, *62*, 6558−6565.

(17) (a) Fry, A. J. *Electrochem. Commun.* **2005**, *7*, 602−606. (b) Macías-Ruvalcaba, N. A.; Evans, D. H. *J. Phys. Chem. B.* **2005**, *109*, 14642−14647.

(18) Barrière, F.; Geiger, W. E. *J. Am. Chem. Soc.* **2006**, *128*, 3980−3989.

(19) (a) Yang, B.; Liu, L.; Katz, T. J.; Liberko, C. A.; Miller, L. L. *J. Am. Chem. Soc.* **1991**, *113*, 8993−8994. (b) Du, S.; Farley, R. D.; Harvey, J. N.; Jeffery, J. C.; Kautz, J. A.; Maher, J. P.; McGrath, T. D.; Murphy, D. M.; Riis-Johannessen, T.; Stone, F. G. A. *Chem. Commun.* **2003**, 1846−1847.

(20) Mao, F.; Tyler, D. R.; Bruce, M. R. M.; Bruce, A. E.; Rieger, A. L.; Rieger, P. H. *J. Am. Chem. Soc.* **1992**, *114*, 6418−6424.

(21) (a) Salaymeh, F.; Berhane, S.; Yusof, R.; de la Rosa, R.; Fung, E. Y.; Matamoros, R.; Lau, K. W.; Zheng, Q.; Kober, E. M.; Curtis, J. C. *Inorg. Chem.* **1993**, *32*, 3895−3908. (b) Neyhart, G. A.; Hupp, J. T.; Curtis, J. C.; Timpson, C. J.; Meyer, T. J. *J. Am. Chem. Soc.* **1996**, *118*, 3724−3729. (c) Sutton, J. E.; Taube, H. *Inorg. Chem.* **1981**, *20*, 3125−3134.

(22) (a) McKee, M. L.; Wang, Z.-X.; Schleyer, P. v. R. *J. Am. Chem. Soc.* **2000**, *122*, 4781−4793. (b) McKee, M. L. *Inorg. Chem.* **2002**, *41*, 1299−1305.

(23) Zhao, Y.; Truhlar, D. *Theor. Chem. Acc.* **2008**, *120*, 215−241.

(24) Frisch, M. J.; Trucks, G. W.; Schlegel, H. B.; Scuseria, G. E.; Robb, M. A.; Cheeseman, J. R.; Scalmani, G.; Barone, V.; Mennucci, B.; Petersson, G. A.; Nakatsuji, H.; Caricato, M.; Li, X.; Hratchian, H. P.; Izmaylov, A. F.; Bloino, J.; Zheng, G.; Sonnenberg, J. L.; Hada, M.; Ehara, M.; Toyota, K.; Fukuda, R.; Hasegawa, J.; Ishida, M.; Nakajima, T.; Honda, Y.; Kitao, O.; Nakai, H.; Vreven, T.; Montgomery, J., J. A.; Peralta, J. E.; Ogliaro, F.; Bearpark, M.; Heyd, J. J.; Brothers, E.; Kudin, K. N.; Staroverov, V. N.; Keith, T.; Kobayashi, R.; Normand, J.; Raghavachari, K.; Rendell, A.; Burant, J. C.; Iyengar, S. S.; Tomasi, J.; Cossi, M.; Rega, N.; Millam, J. M.; Klene, M.; Knox, J. E.; Cross, J. B.; Bakken, V.; Adamo, C.; Jaramillo, J.; Gomperts, R.; Stratmann, R. E.; Yazyev, O.; Austin, A. J.; Cammi, R.; Pomelli, C.; Ochterski, J. W.; Martin, R. L.; Morokuma, K.; Zakrzewski, V. G.; Voth, G. A.; Salvador,

P.; Dannenberg, J. J.; Dapprich, S.; Daniels, A. D.; Farkas, O.; Foresman, J. B.; Ortiz, J. V.; Cioslowski, J.; Fox, D. J. *Gaussian 09*, Revision A.02; Gaussian, Inc.: Wallingford, CT, 2009.
(25) (a) Puiatti, M.; Vera, D. M. A.; Pierini, A. B. *Phys. Chem. Chem. Phys.* **2008**, *10*, 1394−1399. (b) Puiatti, M.; Vera, D. M. A.; Pierini, A. B. *Phys. Chem. Chem. Phys.* **2009**, *11*, 9013−9024.
(26) Lee, T. B.; McKee, M. L. *Inorg. Chem.* **2011**, *50*, 11412−11422.
(27) Barone, V.; Cossi, M. *J. Phys. Chem. A* **1998**, *102*, 1995−2001.
(28) Marenich, A. V.; Cramer, C. J.; Truhlar, D. G. *J. Phys. Chem. B* **2009**, *113*, 6378−6396.
(29) (a) Reiss, H.; Heller, A. *J. Phys. Chem.* **1985**, *89*, 4207−4213. (b) Truhlar, D. G.; Cramer, C. J.; Lewis, A.; Bumpus, J. A. *J. Chem. Educ.* **2004**, *81*, 596−604. (c) Winget, P.; Cramer, C. J.; Truhlar, D. G. *Theor. Chem. Acc.* **2004**, *112*, 217−227. (d) Donald, W. A.; Leib, R. D.; O'Brien, J. T.; Bush, M. F.; Williams, E. R. *J. Am. Chem. Soc.* **2008**, *130*, 3371−3381. (e) Donald, W. A.; Leib, R. D.; Demireva, M.; O'Brien, J. T.; Prell, J. S.; Williams, E. R. *J. Am. Chem. Soc.* **2009**, *131*, 13328−13337. (f) Isse, A. A.; Gennaro, A. *J. Phys. Chem. B* **2010**, *114*, 7894−7899. (g) Kelly, C. P.; Cramer, C. J.; Truhlar, D. G. *J. Phys. Chem. B* **2007**, *111*, 408−422. (h) Tissandier, M. D.; Cowen, K. A.; Feng, W. Y.; Gundlach, E.; Cohen, M. H.; Earhart, A. D.; Coe, J. V.; Tuttle, T. R. *J. Phys. Chem. A* **1998**, *102*, 7787−7794. (i) Tissandier, M. D.; Cowen, K. A.; Feng, W. Y.; Gundlach, E.; Cohen, M. H.; Earhart, A. D.; Tuttle, T. R.; Coe, J. V. *J. Phys. Chem. A* **1998**, *102*, 9308−9308. (j) Fawcett, W. R. *Langmuir* **2008**, *24*, 9868−9875.
(30) Namazian, M.; Coote, M. L. *J. Phys. Chem. A* **2007**, *111*, 7227−7232.
(31) (a) Izutsu, K. *Electrochemistry in Nonaqueous Solutions*; Wiley-VCH: New York, 2002. (b) Diggle, J. W.; Parker, A. J. *Aust. J. Chem.* **1974**, *27*, 1617−1621.
(32) (a) http://webbook.nist.gov/chemistry/ion (accessed Aug 10, 2011). (b) Lias, S. G.; Bartmess, J. E.; Liebman, J. F.; Holmes, J. L.; Levin, R. D.; Mallard, W. G. *J. Phys. Chem. Ref. Data* **1988**, *17*, supplement 1−861.
(33) Boeré, R. T.; Kacprzak, S.; Keßler, M.; Knapp, C.; Riebau, R.; Riedel, S.; Roemmele, T. L.; Rühle, M.; Scherer, H.; Weber, S. *Angew. Chem., Int. Ed.* **2011**, *50*, 549−552.
(34) (a) Bard, A. J.; Faulkner, L. R. *Electrochemical Methods*; John Wiley & Sons, Inc.: New York, 1980. (b) Kleier, D. A. *Inorg. Chem.* **1979**, *18*, 1312−1318.
(35) Pathak, B.; Samanta, D.; Ahuja, R.; Jena, P. *ChemPhysChem* **2011**, 2423−2428.
(36) Gutsev, G. L.; Boldyrev, A. I. *Chem. Phys. Lett.* **1984**, *108*, 250−254.
(37) Zint, N.; Dreuw, A.; Cederbaum, L. S. *J. Am. Chem. Soc.* **2002**, *124*, 4910−4917.
(38) (a) Wiersema, R. J.; Middaugh, R. L. *J. Am. Chem. Soc.* **1967**, *89*, 5078−5078. (b) Knoth, W. H.; Sauer, J. C.; England, D. C.; Hertler, W. R.; Muetterties, E. L. *J. Am. Chem. Soc.* **1964**, *86*, 3973−3983.
(39) Middaugh, R. L.; Wiersema, R. J. *Inorg. Chem.* **1971**, *10*, 423−424.
(40) Wong, E. H.; Kabbani, R. M. *Inorg. Chem.* **1980**, *19*, 451−455.
(41) (a) Grabowski, Z. R.; Rotkiewicz, K.; Rettig, W. *Chem. Rev.* **2003**, *103*, 3899−4031. (b) Shima, S.; Vogt, S.; Gobels, A.; Bill, E. *Angew. Chem., Int. Ed.* **2010**, *49*, 9917−9921. (c) Felton, G. A. N.; Petro, B. J.; Glass, R. S.; Lichtenberger, D. L.; Evans, D. H. *J. Am. Chem. Soc.* **2009**, *131*, 11290−11291.
(42) Speiser, B.; Tittel, C.; Einholz, W.; Schafer, R. *J. Chem. Soc., Dalton Trans.* **1999**, 1741−1752.
(43) (a) Lewis, J. S.; Kaczmarczyk, A. *J. Am. Chem. Soc.* **1966**, *88*, 1068−1069. (b) Power, P. P. *Chem. Rev.* **2003**, *103*, 789−810.
(44) Bowden, W. *J. Electrochem. Soc.* **1982**, *129*, 1249−1252.
(45) Peymann, T.; Knobler, C. B.; Hawthorne, M. F. *J. Am. Chem. Soc.* **1999**, *121*, 5601−5602.
(46) Davan, T.; Morrison, J. A. *Inorg. Chem.* **1986**, *25*, 2366−2372.
(47) Gagné, R. R.; Koval, C. A.; Lisensky, G. C. *Inorg. Chem.* **1980**, *19*, 2854−2855.